Chapter 6
Development and Potential Triggering Mechanisms for a Large Holocene Landslide in the Lower St. Lawrence Estuary

Genevieve Cauchon-Voyer, Jacques Locat, Guillaume St-Onge, Serge Leroueil, and Patrick Lajeunesse

Abstract The Betsiamites 7,250 cal BP submarine landslide mobilized a volume of 1.3 km^3 in the St. Lawrence Estuary, Eastern Canada. The failure was initiated in shallow water between 10 and 140 mbsl and most likely developed in a unit stratified clayey silt deposits following a very strong earthquake. Most of the failed mass appears dislocated and evacuated the failure source area. This paper concludes that gas hydrates dissociation could not have influenced slope stability on the shelves of the Lower St. Lawrence Estuary in the Early Holocene and that despite the high sedimentation rates prior to the failure this condition did not act independently as a significant trigger for the Betsiamites failure.

Keywords Submarine mass movements • Holocene failures • Morphology

6.1 Introduction

In Eastern Canada, submarine landslides have recently received more attention (e.g., Duchesne et al. 2003; Lajeunesse et al. 2007; Campbell et al. 2008; Cauchon-Voyer et al. 2008; Gagné 2008) and their consequences have been

G. Cauchon-Voyer (✉) • J. Locat
Département de géologie et génie géologique, Université Laval, Québec, Québec, Canada G1K 7P4
e-mail: genevieve.cauchon-voyer.1@ulaval.ca

G. St-Onge
Canada Research Chair in Marine Geology, ISMER and GEOTOP, Université du Québec à Rimouski, Rimouski, Québec, Canada G5L 3A1

S. Leroueil
Département de génie civil, Université Laval, Québec, Canada G1K 7P4

P. Lajeunesse
Centre d'études nordiques and Département de géographie, Université Laval, Québec, Canada G1K 7P4

Y. Yamada et al. (eds.), *Submarine Mass Movements and Their Consequences*, Advances in Natural and Technological Hazards Research 31,
DOI 10.1007/978-94-007-2162-3_6,

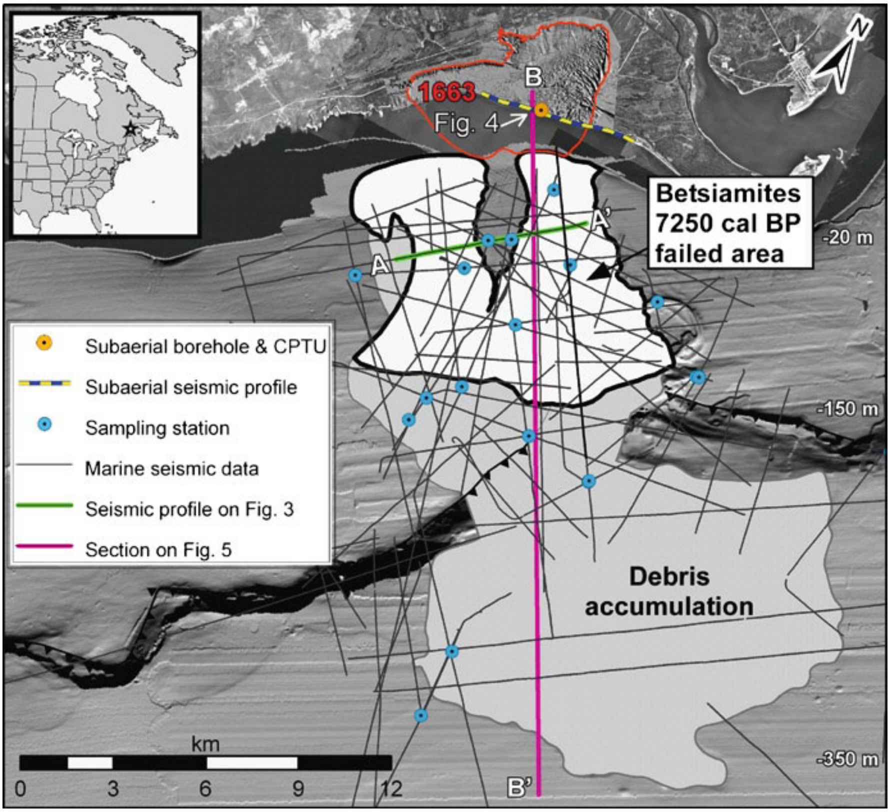

Fig. 6.1 Study site and extent of the Betsiamites landslide scar

summarized (Mosher 2008). The Lower St. Lawrence Estuary is characterized by two ~10 km wide sub-horizontal 2° slope shelves breaking at water depth between 150 and 200 m (Fig. 6.1) where many mass movement scars are observed. The deepest section of the Estuary, the Laurentian Channel at water depth of about between 350 and 375 m, is a long sub-horizontal NE-SW topographic depression.

The North Coast of the St. Lawrence Estuary exhibits areas with subaerial and submarine landslide scars with the largest located on the seafloor off the Betsiamites river delta (Fig. 6.1). This delta was constructed in a time of falling relative sea-level as a result of the melting of the Laurentide Ice Sheet and glacio-isostatic rebound during the Late Wisconsinan, which transported great amounts of sediments from the continent into the Estuary. The Betsiamites landslide complex is the result of at least three distinct landslide events, i.e. the submarine and subaerial Colombier failure in 1663, which extend is indicated on Fig. 6.2, a large failure in 7,250 cal BP and a failure in 9,250 cal BP (Cauchon-Voyer et al. 2011). Morphological analysis of the scar of the 7,250 cal BP landslide event, thereafter

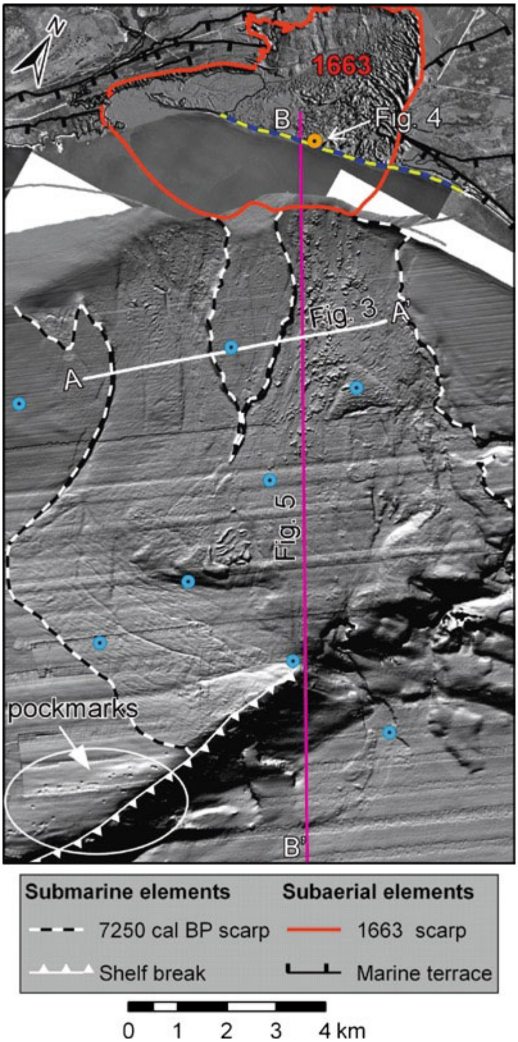

Fig. 6.2 Geomorphology of the Betsiamites scar, see Fig. 6.1 for legend of data source

named Betsiamites slide event, allows establishing that it occurred only in the submarine portion (Cauchon-Voyer et al. 2011) when relative sea-level was about similar to present level (Bernatchez 2003).

6.1.1 Objectives

The 7,250 cal BP Betsiamites submarine slide is the largest scar yet identified on the seafloor of the St. Lawrence Estuary. The main objective of this paper is to describe this massive submarine landslide and discuss its development and potential trigger mechanism.

6.2 Data and Methods

Bathymetric data were acquired using a SIMRAD EM1000 multibeam echosounder. The seismic reflection profiles presented in this study were obtained with an EG&G chirp system (2–12 kHz). Technical details and results on the submarine bathymetric and geophysical data can be found in Cauchon-Voyer et al. (2008). Forty-six sediments samples were recovered in the submarine segment of the delta and the locations of some sampling stations are indicated in Figs. 6.1 and 6.2. In addition, a cone penetration test with pore water pressure measurement (CPTU), providing tip resistance (q_T) and pore pressure measured immediately behind the tip (u_{base}) profiles, which can be compared to hydrostatic condition (u_{hydro}), and a 58 m long borehole (site 46,010) were performed onshore along the current beach (Figs. 6.1 and 6.2). Detailed description of the CPTU and core data analysis and results can be found in (Cauchon-Voyer et al. 2011).

6.3 Morphology of the Betsiamites Slide Complex

The Betsiamites failure developed over an area of 54 km^2 at water depth from −10 mbsl to −140 mbsl (Fig. 6.2) and mobilized about 1.3 km^3 of sediments, leading to an average landslide thickness of 24 m. This scar is made up of two main topographic depressions, the West depression and the East depression, separated by an intact butte with steep flanks (15–20°) and flat top (Figs. 6.2 and 6.3). In the West and East depressions of the scar, the escarpment height ranges from 12 to 20 m above the seafloor. The floor of the landslide scar is overlain by up to 20 m of landslide debris deposits (Fig. 6.3).

Based on core data and seismic profiling, the upper 3–10 m of these landslide debris deposits are associated with subaerial landslide debris resulting from the 1663 Colombier landslide event (Cauchon-Voyer et al. 2011). The intact butte within the central part of the scar extends over 5 km^2 with a maximum length and width of 4.5 and 1.6 km respectively. The average slope of the top of this butte is 1°, which corresponds more or less to the slope of the seafloor prior to failure. In the Laurentian Channel, at water depths between 350 and 375 m, there is a large debris lobe covering an area of 115 km^2 with a maximum diameter of 15 km (Fig. 6.2). With an average thickness of 9 m, the lobe has an estimated volume of 1 km^3.

6.4 Lithostratigraphy and Failure Surface

The lithostratigraphy and the material involved in the 7,250 cal BP Betsiamites slide are mostly assessed on the basis of geophysical surveys (Fig. 6.3) as most of the sediment cores recovered offshore consist of 1,663 landslide debris or post-glacial hemipelagic sediments deposited after the Betsiamites slide. The main challenge for

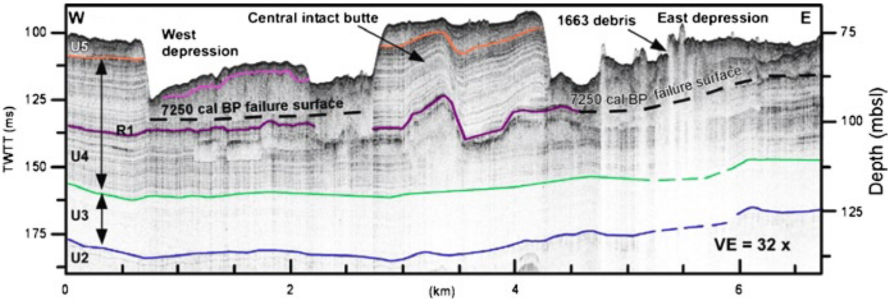

Fig. 6.3 Seismic profile across the Betsiamites landslide scar, along line A–A′, on Fig. 6.2 (Modified from Cauchon-Voyer et al. 2008)

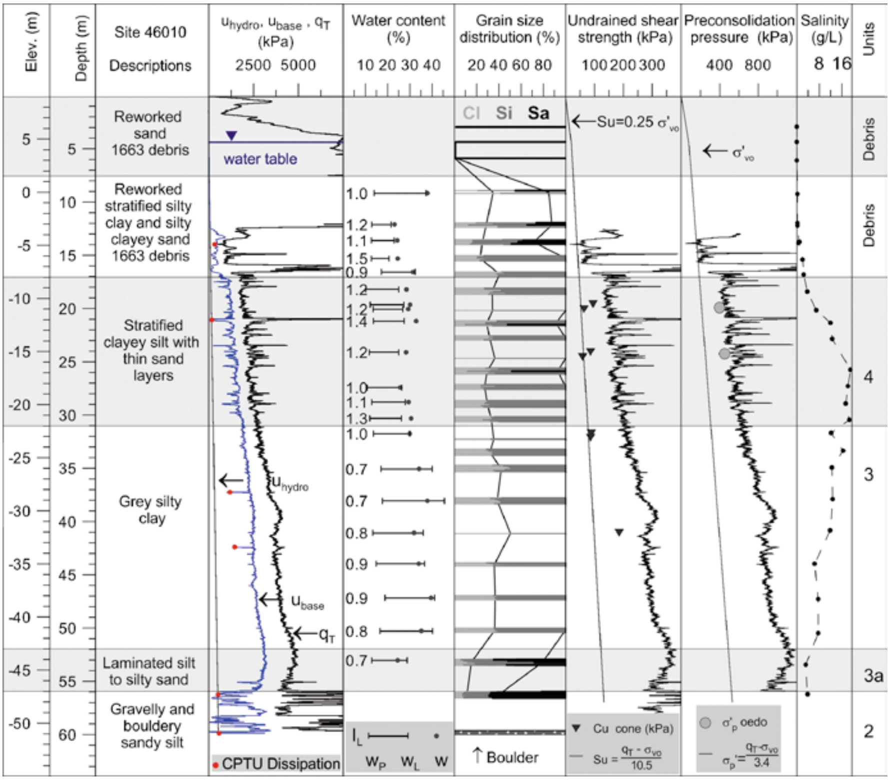

Fig. 6.4 Geotechnical profile carried out onshore along the shoreline (Modified from Cauchon-Voyer et al. 2011). This borehole is located outside the 7,250 cal BP scar but inside 1,663 failure scar. The 7,250 cal BP failure developed within unit 4. Shear strength and preconsolidation pressure profiles are estimated from CPTU results

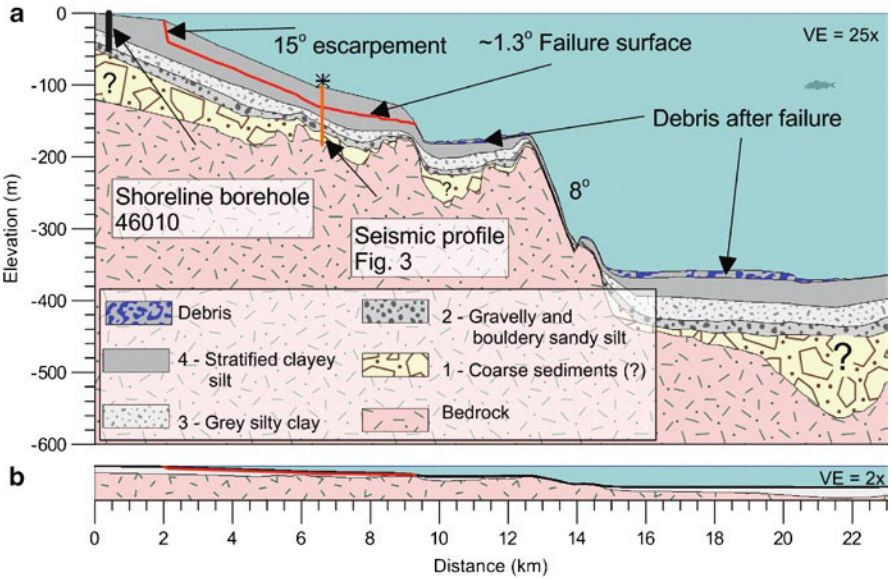

Fig. 6.5 (**a**) Morphostratigraphic reconstitution of the Betsiamites landslide showing the topography prior to failure and the accumulation of debris after failure. See location on Fig. 6.1, profile B–B′. (**b**) Same profile at VE = 2×

offshore work on older landslides is to obtain geological validation and properly evaluate the in situ geotechnical properties. To counter this limitation in this coastal area, a subaerial CPTU and borehole (Fig. 6.4) were carried out along the coastline. six main geotechnical units are identified at this site. The upper two are debris from the 1,663 events. Unit 4 contains many ~5 cm-thick silty layers interbedded in clayey layers. Unit 3 is a homogenous grey silty clay, unit 3a is a thin layer of a laminated silt and unit 2 is a gravelly and bouldery silt.

The seismic profiling shows that the bedrock has an irregular topography and creates a sediment basin at the toe of the failure scar on the shelf (Fig. 6.5). Prior to failure, the sediment layers deposited conformably on the underlying bedrock and allowed for little accumulation of sediments at the toe of the scar (Fig. 6.5). Seismic interpretations (Fig. 6.3) associated with core data (Fig. 6.4) shows that the Betsiamites failure developed in a unit of more than 25 m of stratified clayey silt deposit (Fig. 6.5), labeled 4 (Figs. 6.4 and 6.5) and U4 on the seismic profiles (Fig. 6.3). On average, unit 4 consist of 30% of clay ($d < 2$ μm), 67% of silt ($2 < d < 63$ μm) and 2% of sand (+63 μm).

The failure surface identified from the seismic profiles has a slope angle of about 1.3°. Local and regional chronostratigraphic and paleogeographic work (Bernatchez 2003; St-Onge et al. 2003, 2008; Cauchon-Voyer et al. 2011) shows that the sequence of glaciomarine sediments (units 2–3–4) shown on Fig. 6.3 was deposited approximately in about 4,000 years between 11 and 7 cal ka in a time of significant sea-level fall. These very high sedimentation rates, averaging 15 mm/year, occurred prior to the 7,250 cal BP Betsiamites failure.

6.5 Movement Development

The failure developed along a surface with a low angle of about 1°. According to the geometry of the slope, the failure was likely initiated at the bottom of the mass and propagated upslope (Fig. 6.5).

Most of the failed mass appears to have moved outside the source area. In fact, when comparing the volume of the 54 km^2 scar on the shelf (1.3 km^3) and the volume of the sediment lobe (1 km^3) in the Laurentian Channel, only 20% of the debris remained in the source area and on the shelf. When the landslide mass reached the shelf break, it flowed down to the Laurentian Channel and appears on the seismic profile completely remolded. The height potential, more than 200 m, of the shelf break likely helped the sediments to remold, facilitating the mobility of the mass to create the debris fan. In fact, the material did not accumulate on the 8° slope which would have obstructed the movement and reduced the overall flow of the mass.

6.6 Triggering Mechanisms

The Betsiamites failure developed over more than 8 km in deposits with slope angle of about 1° (Fig. 6.5). To create such a large failure in these conditions, diverse factors could have contributed to the development of the failure, its propagation and the evacuation of the failed mass. The effects of gas and excess pore water pressure resulting from high sedimentation rate or an earthquake are investigated in order to define their potential influence on the development of the Betsiamites failure. As the Betsiamites River had a configuration similar to what it is at present (Fig. 6.1) at the time of the failure (Bernatchez 2003) and the water depth of the scar area range between −10 and −140 m, we assume that significant erosive currents did not form to influence the stability of the area. As the failure developed 7,520 cal BP, is it difficult to assess if groundwater flow influenced the initiation.

Areas with greater amount of pockmarks in the vicinity of the Betsiamites landslides (Fig. 6.2) have been identified (Cauchon-Voyer et al. 2008). The pockmarks in the St. Lawrence estuary have recently been studied and these studies suggest that they formed through the recent and still active release of gas from a reservoir within the Paleozoic sedimentary succession (Pinet et al. 2008, 2009; Lavoie et al. 2010) and thus are not biogenic gas resulting from synchronous sedimentation of organic matter. Such observations led to the questioning that gas could have been a possible trigger for submarine landslides in the St. Lawrence Estuary (Campbell et al. 2008; Cauchon-Voyer et al. 2008; Pinet et al. 2008). Gas can have an effect on seafloor stability if gas hydrates dissociate (Sultan et al. 2004) or if free gas influences the permeability and/or the structure of the sediments (Best et al. 2003). Along the North shelf (water <150 mbsl) of the Estuary where there are many failure scars, we can discard that gas hydrates dissociation acted as a trigger mechanism because the conditions for hydrate formation (mainly pressure and temperature), and thus dissociation, were likely never met following the last deglaciation (Pinet et al. 2008).

Another hypothesis for the origin of this failure would be that the very high sedimentation rates estimated prior to the failure could have generated high pore water pressure. For an average thickness (h) of 24 m of sediments having a buoyant unit weight (γ') of 9.7 N/m^3 deposited on an angle of 1.3°, a simple infinite slope stability analysis indicates that the pore pressure required to bring the slope to failure (FS = 1), if no other mechanisms are involved, correspond to 0.98 of the weight of the sediment layer. This value corresponds to 230 kPa of overpressure, which is extremely high and hence would require that only 2% of dissipation and consolidation have occurred. Such high overpressures are obtained at much greater depth (more than 250 m with rate up to 35 mm/year) with more advanced modeling (Hustoft et al. 2009). This simple demonstration indicates that pore water pressure resulting only from high sedimentation rates likely had the time to dissipate and hence did not play an important role in the development of the Betsiamites failure.

Pore pressures generated by rapid sedimentation might not cause failure on their own but could still contribute to failure through another mechanism, e.g., an earthquake. Earthquakes are known to generate slope failure by degrading the shear strength and increasing the pore pressure within a slope. Such mechanisms likely played an important role in the initial triggering of a failure on such a low slope (1°) for the Betsiamites failure. In fact, shaking could cause significant strength reduction in one or several layers within the stratified unit (labeled U4 on Fig. 6.3). In the case of the Betsiamites failures, more study are required to investigate the cyclic behavior of the sediments involved, but similar demonstration of the influence of stratification on cyclic strength of stratified sand-silt samples were demonstrated (e.g., Konrad and Dubeau 2003; Dan et al. 2009). A related mechanism has been proposed by Kokusho (1999) which suggested that following the earthquake, the water expulsed from the liquefied layer could become trapped between less permeable layers above, which may generate a water film over which the soil mass could start sliding. This mechanism could support the morphological observations within the landslide scar as the deposits were easily transported outside the scar. In fact, to account for the large scar observed on a low slope angle with less than 10 m of debris of the shelf (20%), a significant sliding mechanism must have been involved (Fig. 6.3).

6.7 Concluding Remarks and Future Work

The 7,250 cal BP Betsiamites slide (1.3 km^3 over 54 km^2) is one of the largest landslides in the St. Lawrence Estuary. The failure surface developed in a thick stratified sequence clayey silt. This paper concludes that gas hydrates dissociation could not have influenced slope stability on the shelves of the St. Lawrence Estuary in the Early Holocene. The stability of the slope prior to failure does not appear to have been influenced by excess pore pressures resulting independently from high sedimentation rates as dissipation in the deposits could occur efficiently. The most likely trigger for such a large failure would be excess pore pressures resulting from an earthquake. With a volume of more than 1.3 km^3, it would be important to direct further analysis to determine if this event triggered a tsunami.

Acknowledgments The authors wish to thank the Ministère des Transports du Québec (MTQ), NSERC and FQRNT for their financial support. We thank the MTQ for the permission to use their topographic and LIDAR surveys, borehole, and piezocone soundings data of the Colombier – Betsiamites area. We recognize the contribution of all scientists and crew members on board the Coriolis II, F.G. Creed, and Guillemot vessels. The Canadian Hydrographic Service and GSC-Quebec are also acknowledged for their contribution to bathymetric data acquisition. We thank Homa Lee and Jean-Sébastien L'Heureux for their constructive comments.

References

Bernatchez P (2003) Évolution littorale holocène et actuelle des complexes deltaiques de Betsiamites et de Manicouagan-Outardes: synthèse, processus, causes et perspectives. Université Laval, Québec

Best A, Clayton C, Longva O, Szuman M (2003) The role of free gas in the activation of submarine slides in Finneidfjord. In: Locat J, Mienert J (eds) Submarine mass movements and their consequences 1st international symposium, 2003. Kluwer Academic, Dordrecht, pp 419–498

Campbell C, Duchesne MJ, Bolduc A (2008) Geomorphological and geophysical evidence of Holocene instability on the Southern slope of the Lower St. Lawrence Estuary, Québec. Paper presented at the 4e conférence canadienne sur les géorisques: des causes à la gestion – 4th Canadian conference on geohazards: from causes to management, Québec

Cauchon-Voyer G, Locat J, St-Onge G (2008) Late-Quaternary morpho-sedimentology and submarine mass movements of the Betsiamites area, Lower St. Lawrence Estuary, Quebec, Canada. Mar Geol 251(3–4):233–252

Cauchon-Voyer G, Locat J, Leroueil S, St-Onge G, Demers D (2011) Large-scale subaerial and submarine Holocene and recent mass movements in the Betsiamites area, Quebec, Canada. Eng Geol. doi:10.1016/j.enggeo.2011.04.011

Dan G, Sultan N, Savoye B, Deverchere J, Yelles K (2009) Quantifying the role of sandy–silty sediments in generating slope failures during earthquakes: example from the Algerian margin. Int J Earth Sci 98(4):769–789

Duchesne MJ, Long BF, Urgeles R, Locat J (2003) New evidence of slope instability in the Outardes Bay delta area, Quebec, Canada. Geo-Mar Lett 22(4):233–242. doi:10.1007/s00367-003-0121-6

Gagné H (2008) Géomorphologie et géologie marine du Quaternaire du secteur Trois-Pistoles-Forestville, estuaire du Saint-Laurent (Québec). Université Laval, Québec

Hustoft S, Dugan B, Mienert J (2009) Effects of rapid sedimentation on developing the Nyegga pockmark field: constraints from hydrological modeling and 3-D seismic data, offshore mid-Norway. Geochem Geophys Geosys 10(6):Q06012

Kokusho T (1999) Formation of water film in liquefied sand and its effect on lateral spread. J Geotech Geoenviron Eng ASCE 125(10):817–826

Konrad JM, Dubeau S (2003) Cyclic strength of stratified soil samples. In: Locat J, Mienert J (eds) Submarine mass movements and their consequences 1st international symposium. Kluwer Academic, Dordrecht, pp 47–57

Lajeunesse P, St-Onge G, Locat J, Labbé G (2007) Multibeam bathymetry and morphostratigraphy of submarine gravity flows and slopes failures in the St. Lawrence Gulf and Lower Estuary (Québec, Canada). Paper presented at the submarine mass movements and their consequences

Lavoie D, Pinet N, Duchesne M, Bolduc A, Larocque R (2010) Methane-derived authigenic carbonates from active hydrocarbon seeps of the St. Lawrence Estuary, Canada. Mar Petrol Geol 27(6):1262–1272

Mosher DC (2008) Submarine mass movements: geohazards with far-reaching implications. Paper presented at the 4e conférence canadienne sur les géorisques: des causes à la gestion – 4th Canadian conference on geohazards : from causes to management, Presse de l'Université Laval, Québec

Pinet N, Duchesne M, Lavoie D, Bolduc A, Long B (2008) Surface and subsurface signatures of gas seepage in the St. Lawrence Estuary (Canada): significance to hydrocarbon exploration. Mar Petrol Geol 25(3):271–288. doi:10.1016/j.marpetgeo.2007.07.01

Pinet N, Duchesne M, Lavoie D (2009) Linking a linear pockmark train with a buried Palaeozoic structure: a case study from the St. Lawrence Estuary. Geo-Mar Lett 30(5):517–522. doi:10.1007/s00367-009-0179-x

St-Onge G, Stoner JS, Hillaire-Marcel C (2003) Holocene paleomagnetic records from the St. Lawrence Estuary, eastern Canada: centennial- to millennial-scale geomagnetic modulation of cosmogenic isotopes. Earth Planet Sci Lett 209(1–2):113–130. doi:10.1016/s0012-821x(03)00079-7

St-Onge G, Lajeunesse P, Duchesne M, Gagné H (2008) Identification and dating of a key Late Pleistocene stratigraphic unit in the St. Lawrence Estuary and Gulf (Eastern Canada). Quaternary Sci Rev 27(25–26):2390–2400

Sultan N, Cochonat P, Foucher J, Mienert J (2004) Effect of gas hydrates melting on seafloor slope instability. Mar Geol 213(1–4):379–401